

Triton photodisintegration with realistic potentials*

W. Schadow and W. Sandhas[†]

Physikalisches Institut der Universität Bonn, Endenicher Allee 11-13, D-53115 Bonn, Germany

The photodisintegration of ${}^3\text{H}$ is treated by means of coupled integral equations using separable versions of the Paris and the Bonn potentials in their kernel. The differential cross section for the inverse reaction is obtained via detailed balance. For the latter process good agreement with the data is found when including final-state interaction, meson exchange currents, higher partial waves in the potential, and electric quadrupole contributions in the electromagnetic interaction.

1. INTRODUCTION

We present triton photodisintegration results obtained for the Paris, the Bonn A and Bonn B potentials. Instead of the W -matrix representation [1] employed in our previous calculations [2], we now use the Ernst-Shakin-Thaler (EST) expansion [3] of these two-body inputs: PEST, BAEST and BBEST [4,5]. As in Ref. [2] we are interested in the $\gamma + t \rightarrow n + d$ cross section over an energy range from threshold up to 40 MeV, while other recent investigations are focused primarily on polarization observables at some specific energies [6–8]. We confirm in this way the strong potential dependence in the peak region observed in Ref. [2], as well as the importance of higher subsystem partial waves at energies above the peak region. There the fully converged results obtained in the present calculations lie between the two competing sets of data [9,10]. A strong correlation of the peak heights and the triton binding energies is found. Making use of detailed balance we calculate also the differential cross section for the radiative capture process $p + d \rightarrow \gamma + {}^3\text{He}$. Good agreement between theory and experiment is achieved at 12.1 MeV and 15.3 MeV, when incorporating final-state interaction and p -waves in the potential.

2. THEORY

The Alt-Grassberger-Sandhas (AGS) equations are well known to go over into effective two-body Lippmann-Schwinger equations [11] when representing the input two-body T -operators in separable form. The neutron-deuteron scattering amplitude, thus, is determined by

$$\mathcal{T}(\vec{q}, \vec{q}'') = \mathcal{V}(\vec{q}, \vec{q}'') + \int d^3q' \mathcal{V}(\vec{q}, \vec{q}') \mathcal{G}_0(\vec{q}') \mathcal{T}(\vec{q}', \vec{q}''). \quad (1)$$

*Talk given at the XVth International Conference on Few-Body Problems in Physics (22-26 July 1997, Groningen, The Netherlands)

[†]This work was supported by the Deutsche Forschungsgemeinschaft under Grant No. Sa 327/23-1

Applying the same technique to the above photodisintegration process, an integral equation of rather similar structure is obtained for the corresponding amplitude [12,13],

$$\mathcal{M}(\vec{q}) = \mathcal{B}(\vec{q}) + \int d^3q' \mathcal{V}(\vec{q}, \vec{q}') \mathcal{G}_0(\vec{q}') \mathcal{M}(\vec{q}'). \quad (2)$$

In both equations the kernel is given by an effective neutron-deuteron potential \mathcal{V} and an effective free Green function \mathcal{G}_0 . However, in Eq. (2) the inhomogeneity of Eq. (1) is replaced by an off-shell extension of the photodisintegration amplitude in plane-wave (Born) approximation,

$$B(\vec{q}) = \langle \vec{q} | \langle \psi_d | H_{\text{em}} | \psi_t \rangle. \quad (3)$$

Here, $|\psi_t\rangle$ and $|\psi_d\rangle$ are the triton and deuteron states, $|\vec{q}\rangle$ is the relative momentum state of the neutron, H_{em} denotes the electromagnetic operator. In other words, with this replacement any working program for n - d scattering [14,15] can immediately be applied to the corresponding photoprocess.

The results presented in this contribution are obtained by employing, instead of the W -matrix representation used in [2], the PEST, BAEST and BBEST potentials as input, however, with an improved parametrization by Haidenbauer [19]. The high quality of this input has been demonstrated in bound-state and scattering calculations [16–18].

The electromagnetic operator relevant in the total cross section is, at the low energies considered, essentially a dipole operator. In the differential cross section we also have to include the quadrupole operator. According to Siegert's theorem [20], they are given by

$$H_{em}^{(1)} \sim -i E_\gamma \sum_{i=1}^3 e_i r_i Y_{1\lambda}(\vartheta_i, \varphi_i) \quad \text{and} \quad H_{em}^{(2)} \sim \frac{E_\gamma^2}{\sqrt{20}} \sum_{i=1}^3 e_i r_i^2 Y_{2\lambda}(\vartheta_i, \varphi_i). \quad (4)$$

where, E_γ denotes the photon energy, r_i the nucleon coordinates, e_i the electric charges, and $\lambda = \pm 1$ the polarization of the photon. The triton wave function in (3) has been calculated with a procedure outlined in Refs. [2,21].

3. RESULTS

Table 1 contains the binding energies and components of the three-body wave functions obtained with high-rank EST expansions compared to results calculated with the original interactions. The binding energies for the latter have been calculated with a program by A. Nogga from Bochum. As shown in Table 1 the corresponding results are in very good agreement, which indicates the high quality of the EST calculations. Another criterion for the quality of the wave functions is provided by the norm of the difference between the $|\psi_{\text{EST}}\rangle$, obtained in EST approximation, and the wave function $|\psi_{2d}\rangle$ obtained in a two-dimensional calculation for the original potential, $N = \|\Psi_{\text{EST}} - \Psi_{2d}\|$. In the cases considered here N is always $< 10^{-3}$, which in fact shows the quality of the EST results. For the further calculations we have projected the wave function on 34 channels ($j \leq 4$), i.e. we have taken into account more than 99.6 % of the whole wave function. In our previous calculations we projected on a smaller number of channels. It turned out that this was not enough to get converged results.

Table 1
Binding energies and components of the wave functions.

| $j \leq 2$ | E_T (MeV) | P(S) | P(S') | P(P) | P(D) |
|------------|-------------|--------|-------|--------|-------|
| PEST | -7.369 | 90.138 | 1.420 | 0.0634 | 8.379 |
| Paris | -7.381 | 90.118 | 1.400 | 0.0644 | 8.417 |
| BAEST | -8.285 | 92.592 | 1.236 | 0.0366 | 6.135 |
| Bonn A | -8.294 | 92.595 | 1.232 | 0.0366 | 6.137 |
| BBEST | -8.088 | 91.614 | 1.189 | 0.0476 | 7.149 |
| Bonn B | -8.101 | 91.616 | 1.184 | 0.0482 | 7.152 |

Figure 1 shows the results for the Paris, the Bonn A and the Bonn B potentials compared to the experimental data [9,10,22], the total subsystem angular momentum of the two-body potential being restricted to $j \leq 2$ both in the calculation of $|\psi_t\rangle$ and the treatment of Eq. (2). As observed already in our previous W -matrix approach [2] there is a considerable discrepancy between the Paris and Bonn results in the low energy peak region.

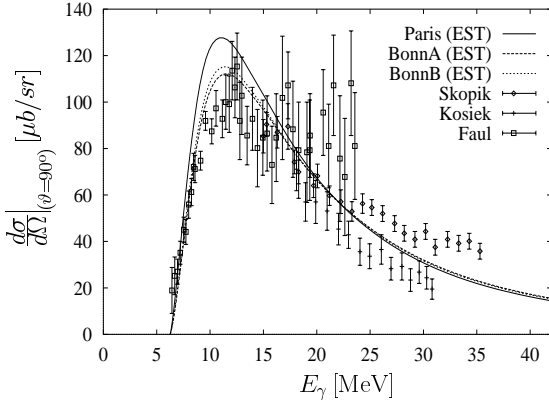


Figure 1. Differential cross section at $\vartheta = 90^\circ$ for $\gamma + {}^3\text{H} \rightarrow n + d$ obtained with the PEST, BAEST and BBEST ($j \leq 2$) potentials. The data are from [9,10,22].

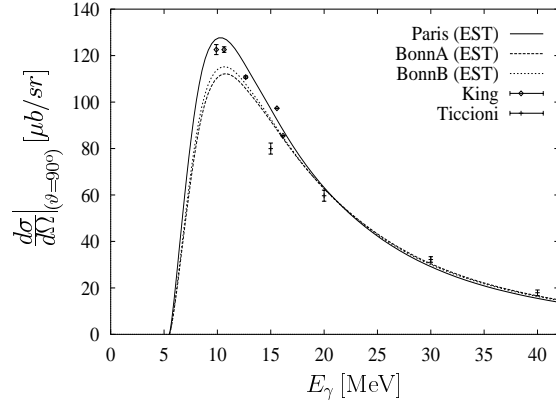


Figure 2. Same as Fig. 1 but for the process $\gamma + {}^3\text{He} \rightarrow p + d$. The data are from [23,24].

Up to 25 MeV the better agreement with the data is achieved for the Bonn potentials. In view of the experimental errors the relevance of this observation is, of course, somewhat questionable. At higher energies the potential dependence vanishes, but in contrast to the not fully converged results of [2], which favored the data by Skopik et al. [10], our curves lie now almost exactly between the two sets of data [9,10]. More accurate low-energy measurements, therefore, appear highly desirable also in this energy region. They would allow us to estimate the quality of the potential models applied in the current calculations, and to clarify the discrepancies between the data of Kosiek et al. [9] and Skopik et al. [10] and our calculations.

Figure 2 shows the theoretical curves of Fig. 1 compared, however, with the experimental data for ${}^3\text{He}$ photodisintegration. Here, the best agreement is achieved for the Paris potential. In both cases the potential which gives a binding energy close to the experimental values agrees best with the data for the photodisintegration. To show that there is a correlation between the binding energy and the height of the peak, we have plotted these values in Figure 3 for different potentials. The results for all potentials with the same number of partial waves are on a straight line. There is one line for the s -wave MT I+III potential and Yamaguchi potentials with different parameters. The r.h.s. straight line concerns the Paris, Bonn A and Bonn B potentials including their higher partial wave contributions, in particular the p - and f -waves. The line in between is the same relationship, however, with the higher partial waves being switched off.

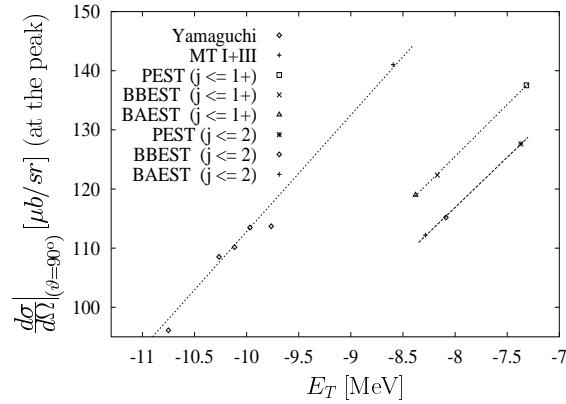


Figure 3. Correlation of the peak heights and the binding energies for different potentials. The result for Malfliet-Tjon (MT I+III) is taken from [2].

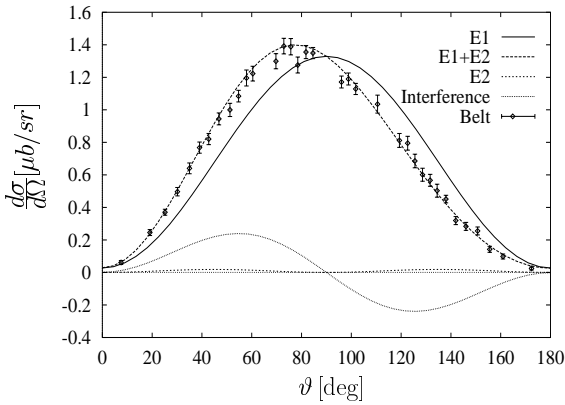


Figure 4. p - d capture for the PEST potential ($j \leq 2$) at $E = 12.1$ MeV. $E1$ - and $E2$ contributions compared to experimental data [25].

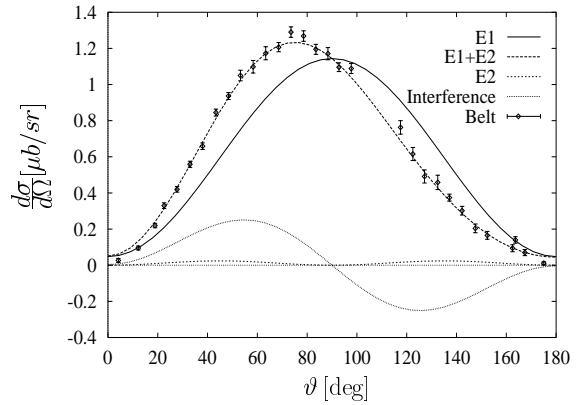


Figure 5. p - d capture for the PEST potential ($j \leq 2$) at $E = 15.3$ MeV. $E1$ - and $E2$ contributions compared to experimental data [25].

Figures 4 and 5 show the differential cross section for p - d radiative capture. Final-state

interaction and meson exchange currents are incorporated and it is seen that electric quadrupole $E2$ contributions are needed to achieve the remarkable agreement between theory and experiment obtained.

REFERENCES

1. E. A. Bartnik, H. Haberzettl, and W. Sandhas, Phys. Rev. C **34**, 1520 (1986).
2. W. Schadow and W. Sandhas, Phys. Rev. C **55**, 1074 (1997).
3. D. J. Ernst, C. M. Shakin, and R. M. Thaler, Phys. Rev. C **8**, 46 (1973); Phys. Rev. C **9**, 1780 (1974).
4. J. Haidenbauer and W. Plessas, Phys. Rev. C **30**, 1822 (1984); Phys. Rev. C **32**, 1424 (1985).
5. J. Haidenbauer, Y. Koike, and W. Plessas, Phys. Rev. C **33**, 439 (1986).
6. J. Jourdan *et al.*, Nucl. Phys. **A453**, 220 (1986).
7. S. Ishikawa, in *Few-Body Systems, Suppl. 6* (Springer-Verlag, Wien, 1992).
8. A. C. Fonseca and D. R. Lehman, in *Proceedings of the 14th International IUPAP Conference on Few-Body Problems in Physics, Williamsburg, VA 1994*, Ed. Franz Gross (AIP, New York, 1995).
9. R. Kosiek, D. Müller, and R. Pfeiffer, Phys. Lett. **21**, 199 (1966).
10. D. M. Skopik, D. H. Beck, J. Asai, and J. J. Murphy II, Phys. Rev. C **24**, 1791 (1981).
11. E. O. Alt, P. Grassberger, and W. Sandhas, Nucl. Phys. **B2**, 167 (1967).
12. I. M. Barbour and A. C. Phillips, Phys. Rev. C **1**, 165 (1970).
13. B. F. Gibson and D. R. Lehman, Phys. Rev. C **11**, 29 (1975).
14. E. A. Bartnik, H. H. T. Januschke, U. Kerwath, and W. Sandhas, Phys. Rev. C **36**, 1678 (1987).
15. Th. Januschke, T. Frank, W. Sandhas, and H. Haberzettl, Phys. Rev. C **47**, 1401 (1993).
16. J. Haidenbauer and Y. Koike, Phys. Rev. C **34**, 1187 (1986).
17. T. Cornelius *et al.*, Phys. Rev. C **41**, 2538 (1990).
18. W. C. Parke, Y. Koike, D. R. Lehman, and L. C. Maximon, Few-Body Systems **11**, 89 (1991).
19. J. Haidenbauer, private communication.
20. A. J. F. Siegert, Phys. Rev. **52**, 787 (1937).
21. L. Canton and W. Schadow, Phys. Rev. C **56**, 1231 (1997).
22. D. D. Faul, B. L. Berman, P. Meyer, and D. L. Olson, Phys. Rev. Lett. **44**, 129 (1980); Phys. Rev. C **24**, 849 (1981).
23. G. Ticcioni, S. N. Gardiner, J. L. Matthews, and R. O. Owens, Phys. Lett. B **46**, 368 (1973).
24. S. King, N. R. Robertson, H. R. Weller, and D. R. Tilley, Phys. Rev. C **30**, 21 (1984).
25. B. D. Belt, C. R. Bingham, M. L. Halbert, and A. van der Woude, Phys. Rev. Lett. **24**, 1120 (1970).